frontiers | Frontiers in Marine Science

TYPE Original Research
PUBLISHED 04 November 2024
DOI 10.3389/fmars.2024.1419953

OPEN ACCESS

EDITED BY
Sudheesh Valliyodan,
Central University of Kerala, India

REVIEWED BY
Birgit Gaye,
University of Hamburg, Germany
Jiaxing Liu,
Chinese Academy of Sciences (CAS), China

*CORRESPONDENCE
Karumuri Ashok
ashokkarumuri@uohyd.ac.in

RECEIVED 19 April 2024
ACCEPTED 17 September 2024
PUBLISHED 04 November 2024

CITATION
Sreejith KS, Sarma VVSS, Pentakota S, Feba F, Hoteit I and Ashok K (2024) Seasonal intensification of oxygen minimum zone: linking Godavari River discharge to fall hypoxia in the Bay of Bengal.
Front. Mar. Sci. 11:1419953.
doi: 10.3389/fmars.2024.1419953

Seasonal intensification of oxygen minimum zone: linking Godavari River discharge to fall hypoxia in the Bay of Bengal

K. S. Sreejith[1,2], V. V. S. S. Sarma[3], Sreenivas Pentakota[1], F. Feba[1], Ibrahim Hoteit[4] and Karumuri Ashok[1,4]*

[1]Center for Earth Ocean and Atmospheric Sciences, University of Hyderabad, Hyderabad, India, [2]Physical Oceangraphy Division, CSIR-National Institute of Oceanography, Panaji, India, [3]CSIR-National Institute of Oceanography-Regional Centre, Visakhapatnam, India, [4]Applied Mathematics and Computational Science, King Abdullah University of Science and Technology, Thuwal, Saudi Arabia

Introduction: This study investigates the biogeochemical impact of Godavari River discharge (GRD) on the Bay of Bengal (BoB), focusing on the formation of an intense and shallow oxygen minimum zone (OMZ) near the river mouth during the fall season. Unlike the BoB's typical intermediate-depth OMZ, this subsurface (~40-200 m) phenomenon is attributed to the interplay of GRD-driven nutrient enrichment, coastal upwelling, enhanced productivity, and subsequent organic matter decomposition.

Data and Methods: Our analysis using the Biogeochemical-Argo floats and World Ocean Atlas 2018 data reveals that a clear shoaling and intensification of the OMZ in the fall season. Further, a comparative analysis at two geographically distinct locations highlighted the pivotal role of GRD.

Results, Discussion, and Implications: The location directly influenced by GRD exhibited significantly higher chlorophyll-a blooms, net primary production during the southwest monsoon, and pronounced oxygen consumption during the fall compared to the other. Our analysis suggests that GRD fuels primary productivity, leading to organic matter abundance and intense oxygen depletion in the subsurface layers, driving the observed shallow OMZ. Understanding the complex interplay between GRD, stratification, upwelling, and biogeochemical processes is crucial for predicting the impact of altered riverine inputs on coastal ecosystems, greenhouse gas emissions, and the overall health of the coastal BoB.

KEYWORDS

Godavari River discharge, oxygen minimum zone, chlorophyll-a, net primary production, decomposition, Bay of Bengal, Argo data

1 Introduction

The Eastern Tropical Pacific (ETP), Arabian Sea (AS), and Bay of Bengal (BoB) are recognized for hosting the most intense oxygen minimum zones (OMZs), characterized by severe hypoxia at intermediate depths (Gilly et al., 2013; McCreary et al., 2013). The formation of these OMZs is attributed to a complex interplay of physical and biogeochemical processes, many of which exhibit commonalities across all three basins. Enhanced primary productivity in surface waters fosters organic matter export to deeper layers. This organic matter undergoes intensified decomposition at intermediate depths, leading to oxygen depletion through microbial respiration (Breitburg et al., 2018; Gilly et al., 2013; Paulmier and Ruiz-Pino, 2009; Pennington et al., 2006). Furthermore, sluggish circulation patterns within these basins limit the advection of oxygen-rich waters into the OMZ, and weak vertical mixing restricts oxygen replenishment from the surface (Breitburg et al., 2018; Gilly et al., 2013; Paulmier and Ruiz-Pino, 2009; McCreary et al., 2013).

The Bay of Bengal oxygen minimum zone (BoB-OMZ) deviates from the typical pattern observed in the ETP and AS despite sharing common drivers for OMZ formation (Gilly et al., 2013; McCreary et al., 2013). This disparity underscores the significant influence of regional factors on the BoB-OMZ's characteristics. A key distinction lies in the primary mechanism responsible for its persistence. Microbial processes such as denitrification and anammox are crucial for oxygen consumption in the ETP and AS (Rao et al., 1994; Gilly et al., 2013; Kalvelage et al., 2013; Castro-González et al., 2014). In contrast, the BoB-OMZ primarily owes its existence to intense salinity stratification (Paulmier and Ruiz-Pino, 2009; Sarma et al., 2018; Udaya Bhaskar et al., 2021). This stratification effectively traps oxygen-depleted waters, hindering vertical mixing and oxygen replenishment from the surface. Cyclonic eddies further influence the intensity and distribution of the BoB-OMZ (Sarma et al., 2018). Interestingly, anticyclonic eddies can sporadically ventilate the BoB-OMZ with oxygen-rich surface waters, leading to temporary weakening and spatial heterogeneity of the hypoxic zone (Sarma and Udaya Bhaskar, 2018). These contrasting mechanisms, absent in the ETP and AS, contribute to the BoB-OMZ's weaker overall intensity and dynamic nature.

The intensity and extent of the BoB-OMZ exhibit significant spatial and temporal variations. In the northern BoB, influenced by major river discharge from the Ganges and Brahmaputra rivers, the summer monsoon and post-monsoon seasons see intensified salinity stratification, leading to a more pronounced OMZ (Howden and Murtugudde, 2001; Jana et al., 2015; Udaya Bhaskar et al., 2021; Sarma et al., 2016). This stratification traps oxygen-depleted waters, hindering vertical mixing and oxygen replenishment. Additionally, the cross-shelf transport of organic matter from the western BoB fuels microbial decomposition, resulting in a stronger OMZ compared to the eastern region (Udaya Bhaskar et al., 2021). Recent studies suggest the possibility of even more intense OMZ formation in the northwestern BoB during winter (Bristow et al., 2017), potentially due to enhanced nutrient input from rivers or atmospheric deposition. However, Sridevi and Sarma (2021) propose that these intense episodes might be transient features caused by eddies. Biogeochemically, the BoB-OMZ is considered weaker compared to other regions. This can be attributed to factors such as weak upwelling, limited primary productivity, and rapid sinking of organic carbon to the deep sea, reducing the availability of organic matter for microbial oxygen consumption (Rao et al., 1994; Ittekkot et al., 1991; Naqvi et al., 1996; Ramaiah et al., 2010; McCreary et al., 2013). Furthermore, several studies suggest that riverine nutrients are rapidly consumed within a limited distance (20 km) from the coast, restricting their contribution to offshore OMZ intensification (Howden and Murtugudde, 2001; Sarma et al., 2018).

The Godavari River, India's third-longest fluvial system (1,465 km), is driven by the monsoon cycle, resulting in concentrated discharge from July to September (Central Water Commission, 2019). This peak discharge coincides with the BoB's highest riverine input, contrasting with the dominance of tidal processes in other seasons (Howden and Murtugudde, 2001; Sarma et al., 2010). While the influence of major rivers such as the Ganges and Brahmaputra on the northern BoB-OMZ is well-established (Jana et al., 2015; Udaya Bhaskar et al., 2021), the annual impact of medium-sized rivers such as the Godavari remains less explored. This study addresses this knowledge gap by investigating the annual cycle of Godavari River discharge (GRD), its potential effects on local coastal primary productivity, and its contribution to the development of a seasonal OMZ near the river mouth. The following section outlines the methodology and details the datasets employed. Section 3 presents our findings on the seasonal evolution of the BoB-OMZ, the biogeochemistry in the river mouth region, and the potential mechanisms driving the intense OMZs observed near the Godavari. Finally, section 4 provides a comprehensive summary and concluding remarks.

2 Data

The GRD data utilized in this study were obtained from the Dowleiswaram barrage, located approximately 50 km upstream of the river's confluence with the BoB. This barrage serves as the final major infrastructure point along the Godavari's course, regulating the downstream flow of freshwater into the BoB. Daily measurements of water released from the Dowleiswaram barrage provided a high-resolution record of GRD variations. These daily values were subsequently aggregated to generate monthly mean time series data spanning 29 years (1990-2018). The use of Dowleiswaram barrage discharge as a proxy for total GRD into the BoB is justified due to several factors. First, the barrage captures the vast majority of the Godavari's freshwater input, as evidenced by minimal tributaries downstream. Second, the relatively short distance (50 km) between the barrage and the BoB minimizes potential losses through evaporation or tributary inputs. This time series data of mean monthly GRD serve as a key foundation for our investigation of the river's influence on coastal BoB dynamics. Due to confidentiality restrictions, the GRD data used in this study were not publicly available. The data was obtained from Superintending Engineer, Irrigation Circle, Dhavaleswaram, Rajamahendravaram, Andhra Pradesh (https://irrigationap.cgg.gov.in/wrd/home; scicbowlm@gmail.com).

This study leverages Biogeochemical-Argo (BGC-ARGO) data, a critical component of the Global Ocean Observing System (Notarstefano, 2020), to provide high-resolution *in situ* station observations in the vicinity of the Godavari River mouth. Within

the extensive BGC-ARGO network, we identified two floats (2902264 and 2902193) strategically positioned within the plume of low-saline GRD. The precise locations of these floats are presented in Figure 1, along with their temporal and location information in Table 1 and Supplementary Tables S1, S2. These two floats provided individual quality-controlled profiles of various oceanographic parameters. Float 2902193 completed 184 data cycles, with three profiles (cycles 49, 59, and 71) acquired within the vicinity of the GRD region through the fall to early winter (mid-September to December). Float 2902264 completed 268 cycles, with three profiles (cycles 41, 44, and 60) in the GRD region through the fall to the winter months (mid-October to January). Both floats were stationed outside the GRD region for the remaining data cycles. Consequently, only the three profiles acquired within the GRD region, as outlined above, were utilized for the analysis of dissolved oxygen (DO), chlorophyll-a (Chl-a) concentration, and particle backscattering coefficient information at 700 nm (bb700) in this study. The DO measurements offer insights into potential oxygen depletion associated with enhanced organic matter decomposition driven by the GRD influx. Chl-a, a proxy for phytoplankton biomass, acts as a marker of primary productivity potentially stimulated by nutrient enrichment from the river discharge. Finally, the particle backscattering coefficient serves as an indicator of the presence and type of suspended particles, including phytoplankton and non-living organic matter, which the GRD dynamics can influence. By scrutinizing these critical variables from the strategically located BGC-ARGO floats, we aim to provide robust observational evidence to confirm and refine our understanding of the Godavari River's impact on the biogeochemical dynamics of the

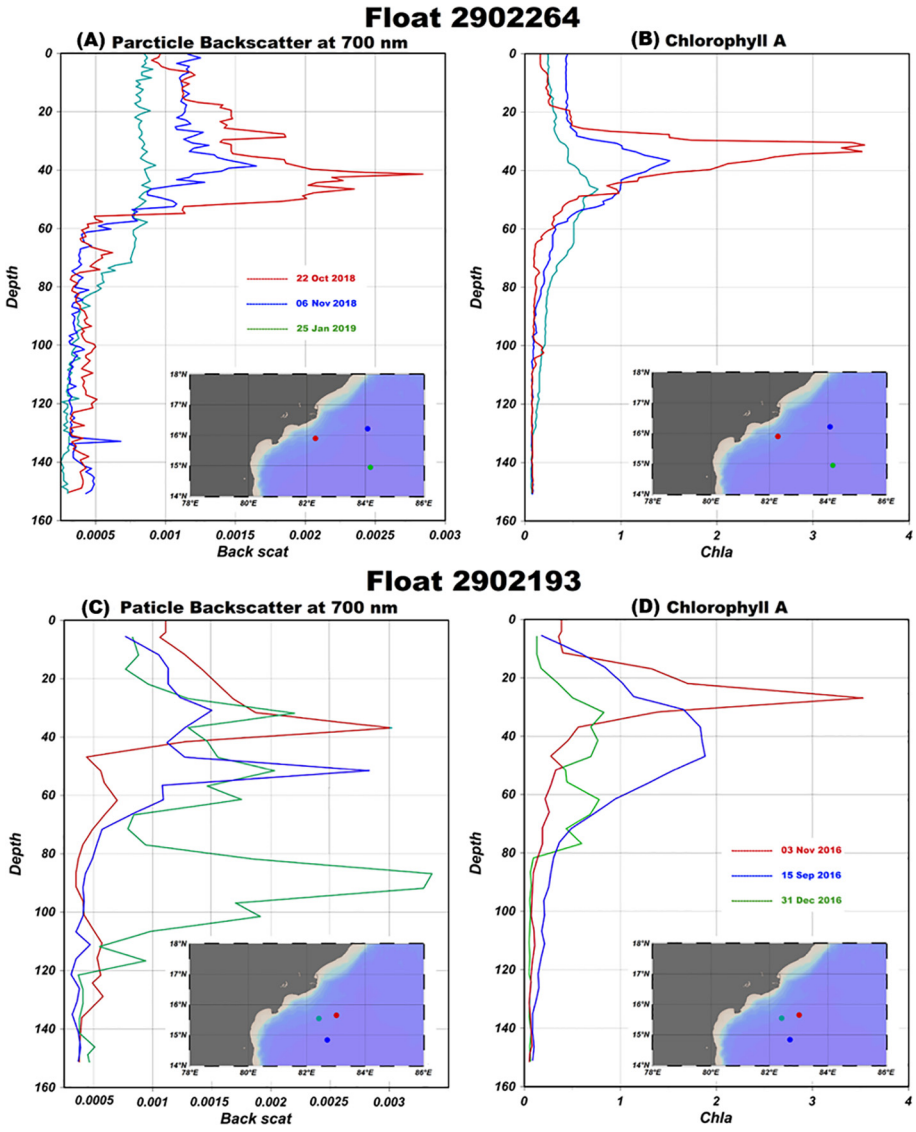

FIGURE 1
Vertical profiles of particle backscatter at 700 nm and CHL-a from BGC-ARGO floats. **(A)** Particle backscatter at 700 nm (m^{-1}) profiles from float 2902264 at 16.01°N, 82.49°E on 22 October 2018, at 16.53°N, 84.16°E on 6 November 2018, and at 14.94°N. 84.2°E on 25 January 2019. **(B)** Same as **(A)** but for CHL-a ($mg.m^{-3}$). **(C)** Particle backscatter at 700 nm (m^{-1}) profiles from float 2902193 at 15.7°N, 83.20°E on 3 November 2016, at 14.83° N, 82.7°E on 15 September 2016, and at 15.54°N. 82.4°E on 31 December 2019. **(D)** Same as **(C)** but for CHL-a ($mg.m^{-3}$).

TABLE 1 Details of BCG-Argo floats used in this study.

WMOID	Maker	Sensors	Start date	End date
2902193	Teledyne, USA	CTD_TEMP, CTD_CNDC, CTD_PRES, OPTODE_DOXY, SCATTEROMETER_BBP, FLUOROMETER_CHLA	27/01/2016	04/07/2018
2902264	NKE, France	CTD_PRES, CTD_TEMP, CTD_CNDC, OPTODE_DOXY, FLUOROMETER_CHLA, BACKSCATTERINGMETER_BBP700	05/04/2018	Till date

coastal BoB region. We obtained BGC-ARGO data from https://biogeochemical-argo.org/data-access.php.

To gain further insights into potential spatial biogeochemical responses to the GRD, we also drew upon complementary datasets from the Ocean Colour Climate Change Initiative (OC-CCI) (https://www.oceancolour.org/browser/index.php?product=chlor_a&page=0&period=monthly&version=1&limit=24&from=2002-01-01&to=2016-01-01&mode=download#results). This fresh initiative provides a robust, merged Level 3 product for monthly mean Chl-a concentrations from 2002 to 2016. This valuable resource utilizes satellite observations from diverse sensors, including Medium Resolution Imaging Spectroradiometer (MERIS), Sea-viewing Wide Field-of-view Sensor (SeaWiFS), Moderate Resolution Imaging Spectroradiometer (MODIS)-Aqua, and Visible Infrared Imaging Radiometer Suite (VIIRS), seamlessly combined to offer a comprehensive and spatially extensive view of phytoplankton biomass across the global ocean (Sathyendranath et al., 2019). The 4 km spatial resolution of the OC-CCI Chl-a data strikes a balance between capturing local dynamics near the Godavari estuary and providing regional context for the observed patterns. To further elucidate the potential impact of GRD on primary productivity, we also leverage monthly mean net primary productivity (NPP) data obtained from the same OC-CCI website for the same timeframe (2002-2016) (https://www.oceancolour.org/browser/index.php?product=pp&page=0&limit=24&from=2002-01-01&to=2016-01-01&mode=browse#results). NPP is estimated using the Ocean Production from the Absorption of Light (OPAL) model. This model builds upon the framework originally proposed by Marra et al. (2003). NPP is integrated over the euphotic zone and expressed in grams of carbon per square meter of sea surface (g C m^{-2}). Four key satellite-derived inputs that are assimilated into OPAL are surface Chl-a concentration, sea surface temperature, photosynthetically active radiation reaching the ocean surface, and the absorption coefficient of colored dissolved organic matter. A detailed description of the NPP calculations is available in O'Reilly (2017). This dataset provides a valuable quantitative estimate of the rate at which organic matter is produced by Chl-a-rich phytoplankton biomass within the coastal BoB region. By analyzing the co-variation between Chl-a, and NPP, we aim to gain insights into the potential stimulation of primary productivity by nutrient enrichment associated with the GRD.

The World Ocean Atlas 2018 (WOA18) serves as a cornerstone resource for this study, providing a comprehensive set of objectively analyzed climatological fields for the world ocean (https://www.ncei.noaa.gov/access/world-ocean-atlas-2018/). These fields, derived from *in-situ* measurements, encompass various oceanographic parameters at standard depth levels across different grid resolutions (5° × 5°, 1° × 1°, and 0.25° × 0.25°). Specifically, the data includes annual, seasonal, and monthly climatologies of temperature, salinity, DO, phosphate, silicate, and nitrate. The annual and seasonal climatologies extend to an impressive depth of 5,500 m, encompassing 102 distinct vertical levels. However, for monthly climatologies, the data extends only up to 1,500 m (57 vertical levels), still providing valuable insights into the temporal dynamics of near-surface ocean processes. Additionally, the chemical parameters (such as DO, phosphate, silicate, and nitrate) are available only on a 5° × 5° and a 1° × 1° horizontal resolution. This choice balances the need for a detailed spatial resolution within the coastal BoB region with the data availability and reliability constraints inherent in monthly climatologies. In this study, we used the monthly climatological salinity (Zweng et al., 2018) on a 0.25° × 0.25° grid, and dissolved oxygen (Garcia et al., 2019) at a 1° × 1° resolution. By leveraging this robust and authoritative dataset, we aim to gain valuable insights into the spatiotemporal patterns of dissolved oxygen and their potential association with the influence of GRD.

The monthly mean horizontal and vertical current data (2000-2020) from the Global Ocean Data Assimilation System (GODAS) developed by the National Centre for Environmental Prediction (NCEP) is used to elucidate the seasonal dynamics of coastal circulation and upwelling near the Godavari River mouth. This advanced reanalysis product (replacing Reanalysis 6) serves as the initial oceanic state for the NCEP's Climate Forecast System (Saha et al., 2006). The GODAS is forced by the momentum flux, heat flux, and freshwater flux. It utilizes a quasi-global configuration of the Geophysical Fluid Dynamics Laboratory (GFDL) MOM.v3 model, encompassing the critical coastal zone with high-resolution grids (1° x 1°, enhanced to 1/3° near the equator) and 40 vertical levels (10 m resolution in the upper 200 m). Leveraging these capabilities of the GODAS data (https://www.cpc.ncep.noaa.gov/products/GODAS/), we estimated the divergence and upwelling of the GRD region. The divergence field represents the net flow of fluid into or out of a specific region and is calculated as the sum of the partial derivatives of the horizontal velocity components (u and v) with respect to x and y, respectively. Positive divergence leads to upwelling as surface water is drawn away, allowing deeper water to rise and replace it.

3 Results and discussion

The monthly distribution of the various physical and biogeochemical fields near the GRD region displays interesting signatures (Supplementary Figures S1–S4). Since a detailed analysis of each month will be too descriptive, we focus on January, April, July, and October to examine the evolution of various fields in the boreal seasons of winter, spring, summer, and fall, respectively.

10.3389/fmars.2024.1419953

3.1 Godavari River discharge and associated biogeochemistry near the river mouth

GRD exhibits a strong seasonality driven by the Southwest Monsoon (SWM) season. Monthly climatology (Figure 2A) reveals a peak discharge exceeding 4700 $m^3.s^{-1}$ in August, coinciding with peak SWM rainfall. Subsequently, GRD declines through September, October, and November, becoming negligible by December. Surface salinity distribution (Figure 2B) generally shows a freshening trend during fall due to the equatorward movement of the West India Coastal Current (WICC) transporting low-salinity waters from the northern BoB. Interestingly, GRD also contributes significantly to this freshening during the SWM season, causing a decrease in over 2 practical salinity units (psu) near the river mouth compared to the pre-monsoon values. From summer to winter, salinity becomes the dominant factor controlling near-surface density stratification. This stratification results in a shallow mixed layer and the formation of a thick barrier layer. The shallow mixed layer restricts the exchange of air-sea fluxes, while the barrier layer suppresses mass and energy exchange between the surface layers and the deeper ocean interior. In short, though the relative contribution of fresh water from GRD is negligible compared to other rivers (Sarma et al., 2016), it has the potential to impact the physical and biogeochemical state of the BoB, especially near the Godavari River mouth region.

GRD profoundly amplifies spatiotemporal Chl-a dynamics in the BoB during the SWM season (Figure 2C). Pre-monsoon and

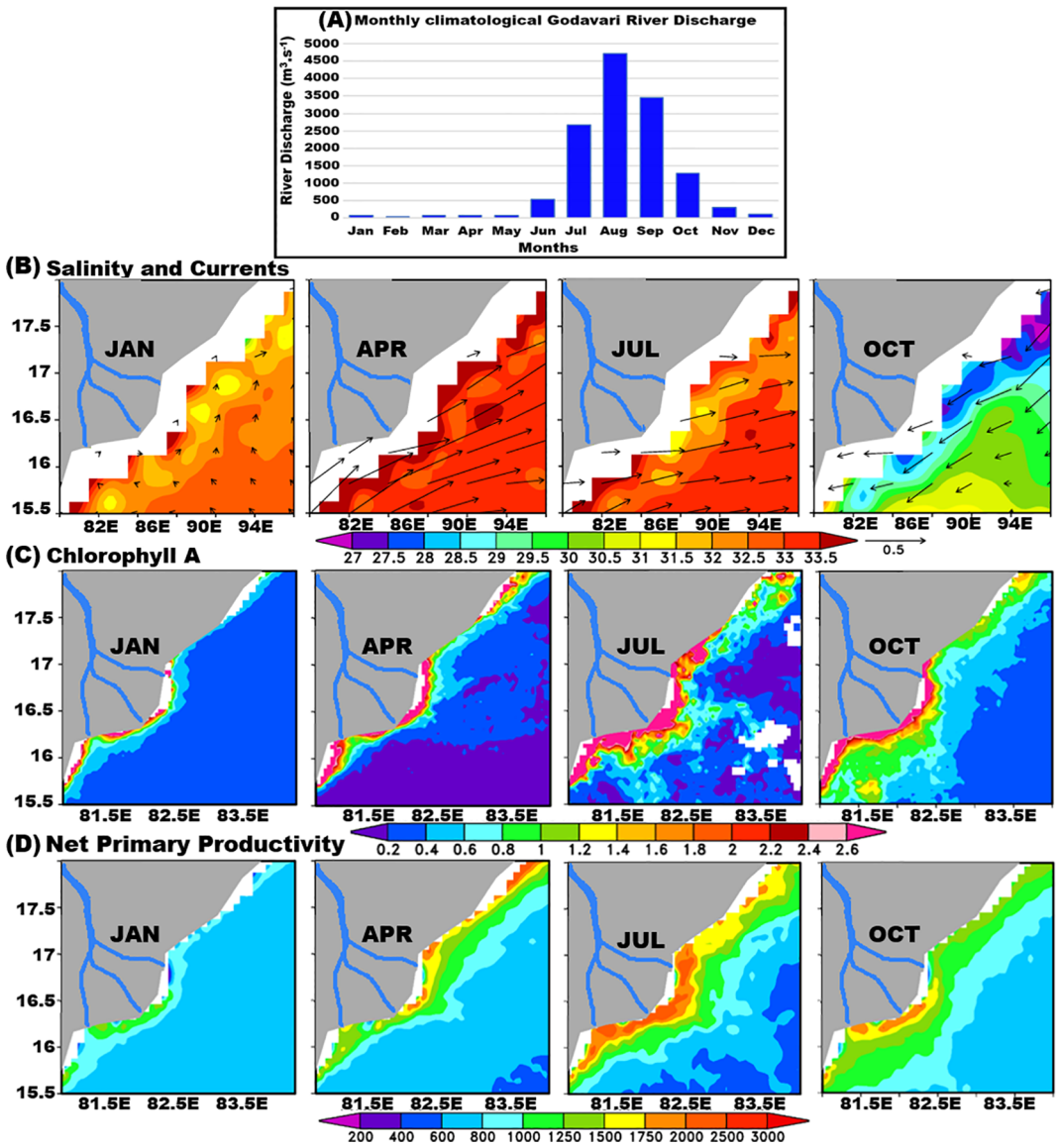

FIGURE 2
(A) Monthly climatology of the collected river discharge data in $m^3.s^{-1}$. **(B)** Surface ocean currents (vector) in $m.s^{-1}$ based on GODAS data over surface salinity (shaded) near the Godavari River discharge region during different seasons. **(C)** Spatial distribution of Chl-a in $mg.m^{-3}$ during different seasons based on OC-CCI data. **(D)** Spatial distribution of NPP in $mgC.m^{-2}$ during different seasons based on OC-CCI data. The Godavari River is schematically represented with the blue contour.

winter months are characterized by Chl-a concentrations lingering well below 0.4 $mg.m^{-3}$, indicative of quiescent phytoplankton growth. In stark contrast, the SWM season ushers in a vibrant pulse of primary productivity, propelling Chl-a to peak values exceeding 2.2 $mg.m^{-3}$ within a significantly expanded spatial footprint encompassing regions up to 83°E around the river mouth (Figure 2C). This pronounced Chl-a bloom intricately mirrors the fluctuations in GRD, diminishing in intensity as the monsoon recedes. The riverine influx of nutrients orchestrates this dramatic seasonal spectacle, directly fueling phytoplankton proliferation and consequently boosting regional NPP, as depicted in Figure 2D. NPP exhibits a gradual ascent from April that culminates at the onset of SWM, and surges beyond 1000 $mgC.m^{-2}$ by July. However, with the waning of the monsoon and subsequent decline in GRD, NPP undergoes a steep drop, leaving the river mouth region with markedly reduced productivity by October. Thus, the annual peak in GRD serves as a potent force, not only inducing vertical stratification but also transforming the BoB into a highly productive ecosystem during the SWM season.

The thriving phytoplankton blooms fueled by enhanced nutrients from the Godavari River are projected to contribute to a significant suspension of organic matter in subsurface BoB waters. To gain insights into this process, we utilized particle backscatter data from two BGC-ARGO floats (2902264 and 2902193) deployed near the river mouth (Figure 1). These floats offered three individual profiles spanning the SWM to winter seasons, allowing us to analyze the organic matter dynamics across contrasting productivity regimes. Details of the data acquisition and processing are provided in Table 1. The BGC-ARGO float 2902264 revealed a pronounced peak in particle backscatter (>0.002 m^{-1}), coinciding with elevated Chl-a concentrations (>3.5 mg m^{-3}) at depths between 30 and 50 m in October 2018 (Figures 1A, B). This peak, located at a depth of 40-50 m, suggests a substantial abundance of organic matter during peak productivity. By November, the intensity of the particle backscatter peak diminished to 0.00165 m^{-1} at 39 m, accompanied by a reduction in Chl-a to 1.5 $mg.m^{-3}$ at 37 m. This decline implied a weakening of organic matter abundance as productivity decreased. Notably, while the extreme particle backscatter peaks were absent by January 2019, Chl-a exhibited a secondary peak at 48 m, albeit with a lower magnitude (<0.8 $mg.m^{-3}$). This suggests a potential decoupling between Chl-a and organic particle suspension during this period.

Data from BGC-ARGO float 2902193 qualitatively support the observed patterns from float 2902264 (Figures 1C, D) in the upper 80 m of the water column. The highest values for both particle backscatter (>0.003 m^{-1}) and Chl-a (>3.5 $mg.m^{-3}$) were observed during November 2016 (late fall/early winter season) at depths between 25 and 40 m. The peak particle backscatter (>0.003 m^{-1}) occurred at 38 m, while the peak Chl-a (>3.5 $mg.m^{-3}$) was slightly shallower at 28 m. These elevated values suggest an enhanced production and possible export of organic matter during the fall, following the peak productivity of the SWM. However, the September 2016 data showed lower particle backscatter (<0.0028 m^{-1}) and significantly reduced Chl-a (<1.9 $mg.m^{-3}$), indicating weaker organic matter suspension preceding the fall peak. Interestingly, while December 2016 exhibited the highest particle backscatter value (>0.0032 m^{-1}) between 85 and 95 m, Chl-a concentrations remained very low (<1 $mg.m^{-3}$) at depths between 30 and 80 m. This discrepancy suggests a potential decoupling between particle export and phytoplankton biomass at deeper depths during this period. Thus, our analysis of the BGC-ARGO data from both floats indicates a seasonal pattern of enhanced Chl-a inducing an elevated particle backscatter underneath it, along with increased organic matter abundance near the Godavari River mouth region, particularly at depths between 25 and 55 m during the fall season. Furthermore, this abundance appears to be linked to elevated Chl-a and NPP during the preceding SWM season.

Hence, GRD significantly impacts the river mouth region during the SWM season through a multifaceted interplay of stratification, primary productivity, and organic matter abundance. The pronounced stratification resulting from a shallow mixed layer and a thick barrier layer generated by GRD restricts vertical mixing, potentially minimizing DO transport from the surface to subsurface layers. Simultaneously, the riverine influx of nutrients fuels phytoplankton growth, leading to enhanced Chl-a concentrations and culminating in elevated NPP. This primary productivity surge drives organic matter export into subsurface layers, potentially capable of influencing DO distribution through microbial decomposition processes. In conclusion, the combined effects of altered stratification, intensified primary productivity at the surface, and organic matter sinking into subsurface layers during the post-SWM season are likely to significantly modify the DO distribution (both horizontal and vertical) near the Godavari River mouth region.

3.2 Dissolved oxygen and seasonal evolution of the OMZ near Godavari River discharge region

The region near the Godavari River mouth lies within the BoB-OMZ, a persistent feature characterized by year-round hypoxic conditions at intermediate depths (200-1,000 m). This section focuses on the potential impact of enhanced organic matter sinking during the SWM and early fall seasons on the distribution of DO and the dynamics (intensity and upper limit) of the BoB-OMZ in the Godavari River mouth region. Analysis of DO profiles from BGC-ARGO floats near the Godavari River mouth reveals the presence of an OMZ (DO within 0-0.5 $ml.l^{-1}$) between 50 to 800 m (average depth levels), with a dynamic response to seasonal changes in organic matter input (Figure 3). Both floats exhibit a shoaling and intensification of the OMZ during the fall season, indicating a potential influence of riverine flow on DO consumption. At float 2902264, the upper limit of the OMZ deepened from 40-45 m in October 2018 (DO ~ 0 $ml.l^{-1}$) to 50 m in November (DO ~ 0.2 $ml.l^{-1}$) and to 100 m by January 2019 (DO ~ 0.5 $ml.l^{-1}$) (Figure 3A). This pattern suggests a gradual deepening of the OMZ as surface productivity declined and oxygen consumption in subsurface layers for microbial respiration reduced. Float 2902193 exhibited a similar trend, with the upper OMZ boundary at 35-40 m in November 2016 (following the SWM with a DO of ~ 0 $ml.l^{-1}$), which was as deep as 75 m in September (pre-SWM with a

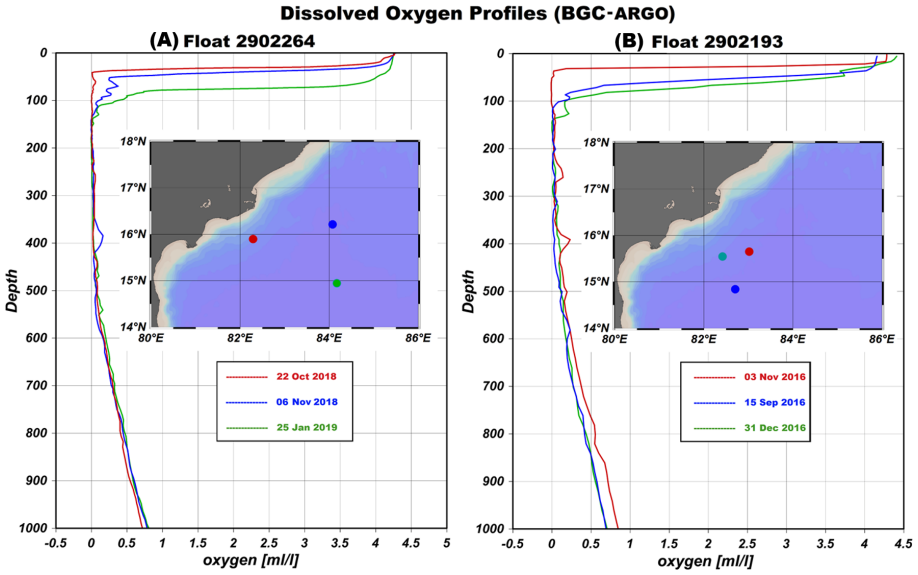

FIGURE 3
Dissolved oxygen (ml.l^{-1}) profiles from BCG-ARGO data. **(A)** Dissolved oxygen profiles from float 2902264 at 16.01°N, 82.49°E on 22 October 2018, at 16.53°N, 84.16°E on 6 November 2018, and at 14.94°N. 84.2°E on 25 January 2019. **(B)** Dissolved oxygen profiles from float 2902193 at 15.7°N, 83.20°E on 3 November 2016, at 14.83°N, 82.7°E on 15 September 2016, and at 15.54°N. 82.4°E on 31 December 2019.

DO of ~ 0.2 ml.l^{-1}) and further down to 105 m in December (with a DO of ~ 0.2 ml.l^{-1}) (Figure 3B). These observations collectively suggest a significant shoaling and intensification of the OMZ near the Godavari River mouth during the fall season. Thus, the enhanced Chl-a and particle backscatter (between 25 and 55 m depth) during the fall season driven by GRD (Figure 1) coincides with shoaling and intensification of the OMZ near the Godavari River mouth. This provides strong evidence for the potential impact of high organic matter sinking on the dynamics of the BoB-OMZ.

The limited availability of BGC-ARGO observations in the GRD region restricts our ability to investigate the seasonal evolution of DO. Therefore, we turn to the objectively analyzed WOA18 DO data, despite its coastal data gap. WOA18 offers sufficient coverage (>80% data availability) for a 63-year period (1955-2017), enabling seasonal analysis of various ocean fields. Figures 4A–D display the vertical distribution of DO (surface to 500 m) in the BoB near GRD (16.8°N) during different seasons, derived from WOA18. High DO concentrations (>4-5 ml.l^{-1}) characterize the basin's surface layers (~0-80 m) year-round. Below this, the OMZ prevails, with its upper boundary primarily residing between 80-200 m, exhibiting seasonal and spatial variations. Winter and spring months reveal similar spatial patterns of the OMZ (Figures 4A, B), with its upper limit confined between 80-110 m depth. A pronounced OMZ (DO < 0.3 ml.l^{-1}) persists below 500 m throughout these seasons. Summer (July) exhibits distinct spatial patterns from the previous two seasons (Figure 4C). Except for a narrow depth range (200-250 m, 92.5-93.5°E), DO levels below the mixed layer generally remain above 0.2 ml.l^{-1}. Additionally, the OMZ upper boundary in the western basin deepens to 110-130 m. The fall season witnesses the most profound OMZ expansion and intensification near the western basin, where the Godavari River discharges (Figure 4D). DO levels below 0.1 ml.l^{-1} appear between 60-175 m in this region, a stark contrast to summer values of 1-1.5 ml.l^{-1} (Figure 4C).

The shoaling and intensification of the OMZ at subsurface depths (40-200 m) near the Godavari River mouth, evident in the BGC-ARGO and WOA18 data during fall, necessitates further investigation. To validate this localized phenomenon, we delved deeper into the seasonal evolution of DO within this critical depth range (40-200 m) in the western BoB (Figures 4E–H). Winter reveals a clear influx of highly oxygenated water from the southern BoB (Figure 4E), aided by the prevailing ocean current system (Figure 2B). This influx maintains sufficient DO (>1 ml.l^{-1}) in the western BoB throughout winter and spring (Figures 4E, F). Even in summer (July) (Figure 4G), subsurface DO (averaged over 40-200 m) near the Godavari River mouth remains moderate, exceeding 1.2 ml.l^{-1}. However, a dramatic shift occurs in the fall (October) as the region transforms into an oxygen-depleted zone (<0.5 ml.l^{-1}) (Figure 4H). This stark contrast highlights the dynamic seasonal cycle of subsurface DO in the western BoB. While oxygenated waters prevail near the Godavari delta basin during winter, spring, and summer, a localized and intense OMZ establishes itself near the river mouth during fall. Thus, coinciding with the retreat of the SWM season, the confluence of increased organic matter input from the Godavari River and enhanced stratification likely contributes to the generation of an intense and shallow subsurface OMZ (40-200 m) near the river mouth.

3.3 OMZ dynamics in the western BoB near the Godavari River mouth

The genesis and dynamics of the pronounced subsurface OMZ observed near the GRD region after the retreat of the SWM season

10.3389/fmars.2024.1419953

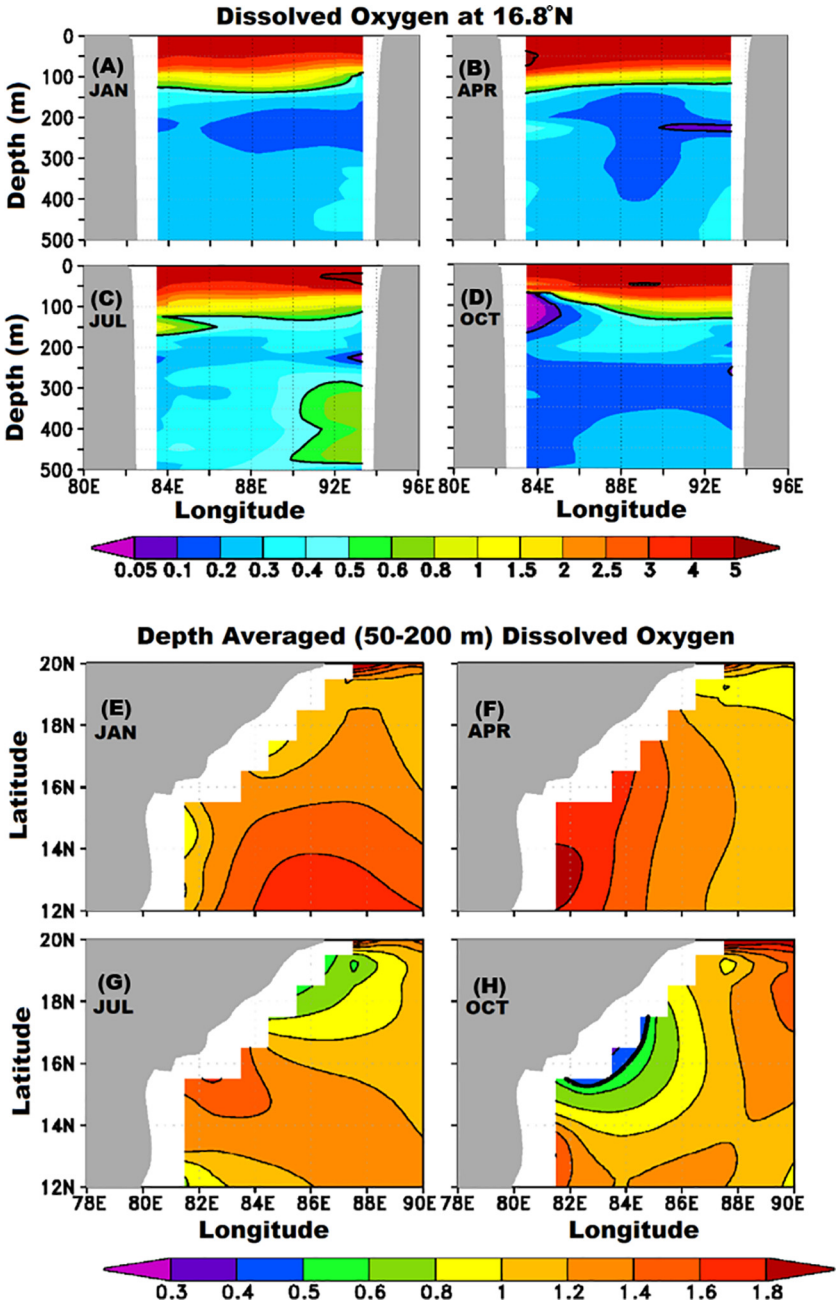

FIGURE 4
(A-D) Vertical section (0-500 m) of dissolved oxygen (ml.l^{-1}) at the Godavari River mouth region (16.8°N) during January (winter), April (spring), July (summer), and October (fall) based on WOA18 data. **(E-H)** Spatial distribution of depth averaged (40-200 m) dissolved oxygen (ml.l^{-1}) near the Godavari River mouth region during different seasons [same as **(A-D)**] based on WOA18 data.

are likely influenced by a complex interplay of physical and biogeochemical factors. In this section, we focus on analyzing other processes such as surface ocean circulation and divergence in the western BoB near the GRD region (Figure 5) using GODAS data, recognizing their crucial role in upwelling and associated biogeochemical processes influencing OMZ dynamics. The surface circulation in the western BoB exhibits distinct seasonal patterns near the Godavari River mouth, playing a crucial role in regional upwelling and potentially influencing the observed OMZ dynamics. The pre-Southwest Monsoon and SWM seasons are characterized by strong northward coastal currents and an eastward current across the BoB, as shown in Figures 5B, C, respectively. Additionally, during the SWM season, south-westerly winds induce positive divergence along the western BoB coast, favoring coastal upwelling (Figure 5C). Following the retreat of the SWM season, the strong monsoon currents subside, and southward-moving coastal currents dominate the western BoB (Figure 5D). This shift creates favorable conditions for upwelling near the GRD region and northwards, indicated by positive surface divergence (Figure 5D). Winter (January) sees a further weakening of the

southward current, and positive divergence persists near the GRD region, suggesting continued upwelling potential (Figure 5A). Thus the oceanic region near the GRD experiences favorable conditions for upwelling throughout the SWM, fall, and late winter periods due to the combined influence of surface currents and divergence. This sustained upwelling could potentially contribute to the observed surge in chlorophyll-a (Chl-a), NPP, and the subsequent intensification and vertical expansion (shoaling) of the OMZ observed after the retreat of the SWM season.

To provide insights into the interplay between GRD and upwelling in shaping dissolved DO and OMZ dynamics in the BoB, we selected two geographically distinct study regions. Box A (82-84°E, 15.5-17°N) lies directly at the Godavari River mouth, maximizing its exposure to GRD influence and benefiting from favorable upwelling conditions during the SWM season. In contrast, Box B (84-86°E, 17-18.5°N), located slightly north, experiences minimized GRD influence while retaining similar upwelling conditions during the SWM season. This strategic selection allows for a comparative analysis, disentangling the individual and combined effects of GRD and upwelling on DO and OMZ dynamics. Figure 6 represents the seasonal evolution of vertical velocity (GODAS data), and those of Chl-a (OC-CCI data), NPP (OC-CCI), and depth-averaged (40-200 m) dissolved oxygen (WOA18 data) in these two selected oceanic regions. The analysis unfolds similar qualitative patterns for vertical velocity (upwelling) in both boxes. In both the oceanic regions, upwelling increases with the emergence of the SWM season and starts declining with its withdrawal. In comparison, Box A records higher values for upwelling than Box B (Figure 6A). The highest upwelling was recorded in July in both boxes, 0.72×10^{-5} m.s^{-1} in Box A and 0.58×10^{-5} m.s^{-1} in Box B. The increase in upwelling during the SWM season clearly reflects the seasonal evolution of Chl-a in Box A, whereas Box B shows a slight decreasing trend from June to July, although it maintained an overall increasing trend during the SWM season (Figure 6B). Both the regions reflected mild Chl-a values during rest of the year. In comparison, Chl-a blooms in Box A (0.8-0.9 mg.m^{-3}) were almost twice as intense as Box B (0.4-0.5 mg.m^{-3}) during the SWM season. NPP also showed a similar seasonal signature (Figure 6C). Both boxes highlighted an increasing trend in NPP during the SWM season and showed similar patterns during the rest of the year. Similar to the Chl-a distribution, Box A recorded very high (> 1100 mgC.m^{-3}) NPP distribution compared to Box B (< 850 mgC.m^{-3}) during the SWM season. The rise in Chl-a and NPP during the SWM season significantly impacted seasonal DO fluctuations in both study regions (Figure 6D). While DO exhibited a mildly increasing trend in both boxes during late winter and pre-monsoon, it displayed a substantial decline with the onset of the SWM season. In Box A, DO plummeted from 3 ml.l^{-1} in May to a critical low of 0.1 ml.l^{-1} in October (fall), representing a drastic decrease of 2.9 ml.l^{-1}. In contrast, Box B experienced a smaller

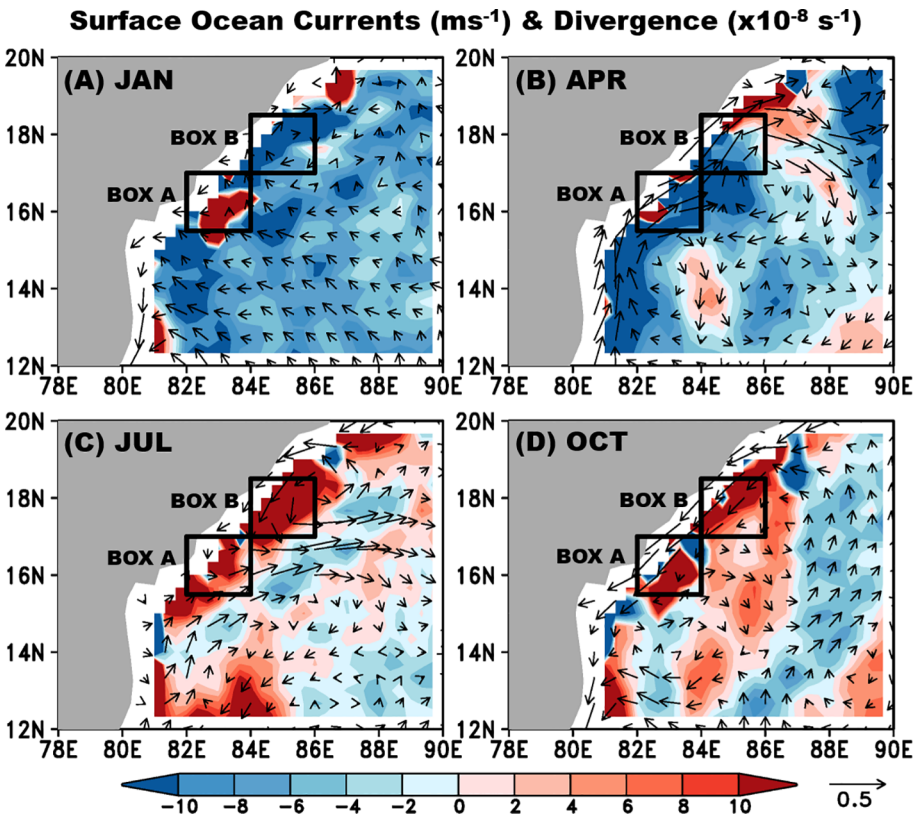

FIGURE 5
(A-D) Surface ocean current (vector) over divergence (shaded) in the west coast of BoB during January (winter), April (spring), July (summer), and October (fall) based on GODAS data. BOX A (82-84°E, 15.5-17°N) and BOX B (84-86°E, 17-18.5°N) are highlighted as rectangular boxes.

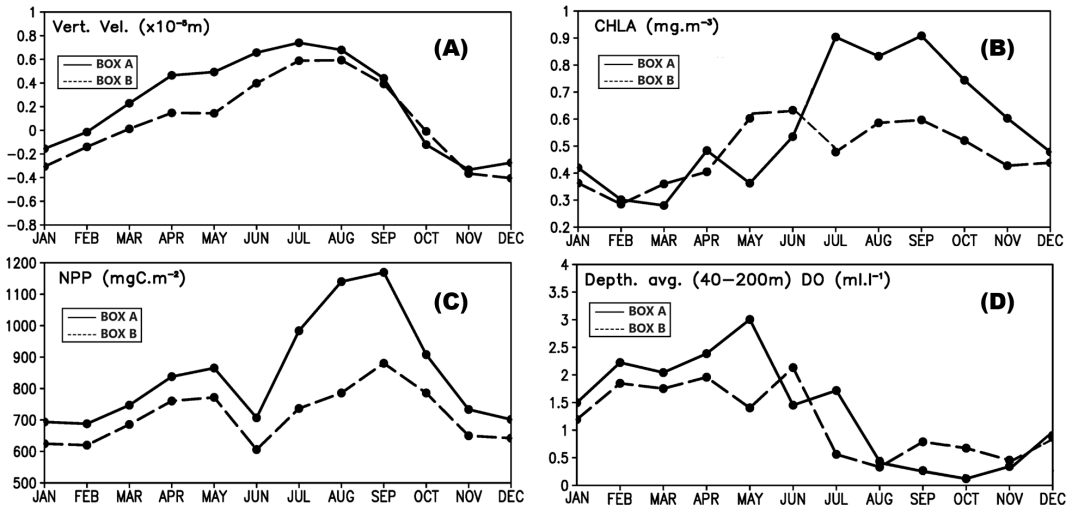

FIGURE 6
(A) Monthly variations of vertical velocity (x 10^{-5} $m.s^{-1}$) area averaged in BOX A (82-84°E, 15.5-17°N) and BOX B (84-86°E, 17-18.5°N) based on GODAS data. **(B)** Same as **(A)** but for Chl-a ($mg.m^{-3}$) based on OC-CCI data. **(C)** same as **(A)** but for NPP ($mgC.m^{-2}$) based on OC-CCI data. **(D)** same as **(A)**, but for depth averaged (40-200 m) dissolved oxygen ($ml.l^{-1}$) based on WOA18 data.

decline, with DO decreasing from 2.2 $ml.l^{-1}$ in June to an average of 0.55 $ml.l^{-1}$ during fall (September-November), representing a decrease of 1.75 $ml.l^{-1}$. In conclusion, it is evident that SWM-driven biogeochemical activity was significantly enhanced in Box A, directly influenced by GRD, leading to pronounced oxygen consumption during fall. This comparative analysis highlights the crucial role of GRD in shaping DO and OMZ dynamics in the BoB.

4 Summary and conclusions

This study delves into the profound biogeochemical impact of GRD in the BoB, with a particular focus on the region near the river mouth. Our key finding is the intriguing presence of an intense and shallow OMZ within the subsurface (40-200 m) depths near the Godavari River mouth during the post-monsoon season which has hardly been mentioned previously. Notably, this phenomenon differs from the conventional intermediate-depth BoB-OMZ prevalent in the basin (McCreary et al., 2013). The temporal evolution of this shallow OMZ was elucidated through data from two BGC-ARGO floats located close to the river discharge region. Their observations revealed a clear intensification and shoaling of the OMZ during fall. To unveil the spatial extent and context of this phenomenon, we leveraged the broader coverage of WOA18 data, facilitating comparisons with other crucial variables. Furthermore, to disentangle the relative influence of GRD and upwelling on OMZ dynamics, we conducted a comparative analysis in two geographically distinct locations. This comparative analysis proved the pivotal role of GRD in shaping the biogeochemical environment near the river mouth. Despite both regions experiencing similar upwelling patterns, the area directly influenced by GRD exhibited significantly higher Chl-a blooms, enhanced NPP during the SWM season, and a more pronounced oxygen consumption during fall. These observations strongly suggest that the extensive nutrient influx from GRD fuels increased primary productivity, leading to enhanced organic matter suspension and subsequent oxygen depletion in the subsurface layers, culminating in the observed intense and shallow OMZ.

Our findings paint a compelling picture of the substantial influence of GRD on BoB biogeochemistry, particularly in the vicinity of the river mouth. Briefly, during the SWM season, the influx of nutrients from GRD, combined with enhanced coastal upwelling, creates favorable conditions for phytoplankton blooms. These blooms, peaking in August and September, are characterized by high Chl-a concentrations and lead to a surge in NPP. However, this elevated productivity comes with a subsequent cost. As the blooms senesce and decompose by fall, an elevation in suspended organic matter at the subsurface depths (40-200 m) develops. This organic matter fuels the activity of heterotrophic microbial communities, leading to intense oxygen consumption through respiration. This microbial respiration, coupled with the reduced atmospheric oxygen supply due to strong stratification, drives the shoaling and intensification of the OMZ off the Godavari River mouth. Understanding and quantifying these impacts are crucial for various reasons. First, alterations in GRD can directly affect primary productivity and food webs in the coastal zone. Second, changes in the OMZ's intensity can influence the release of greenhouse gases such as CO_2 and N_2O, potentially impacting global climate change. Finally, understanding the dynamic interplay between riverine inputs, upwelling, and biogeochemical processes is critical for predicting and managing the future state of the BoB ecosystem. In summary, although the discharge of the Godavari River is negligible compared to other rivers flowing into the BoB, GRD plays a pivotal role in shaping the biogeochemistry of the bay, with profound impacts on primary productivity, oxygen dynamics, and

greenhouse gas emissions. Further research is needed to fully understand the intricate interactions between GRD, upwelling, and biogeochemical processes, and to predict the consequences of future alterations in riverine inputs on this vital ecosystem. It should, however, be noted that the interpretations derived from our analysis are subject to the limited temporal and spatial sample extent, which precludes us from any statistical significance test of the results. We are in the process of initiating a few high-resolution sensitivity experiments with the ocean model that will be 15-20 years long. The outputs will enable us to quantify the contributions of each parameter separately.

Data availability statement

The original contributions presented in the study are included in the article/Supplementary Material. Further inquiries can be directed to the corresponding author.

Author contributions

KS: Conceptualization, Data curation, Formal analysis, Methodology, Software, Writing – original draft, Writing – review & editing. VS: Funding acquisition, Resources, Supervision, Validation, Writing – review & editing. SP: Funding acquisition, Project administration, Resources, Supervision, Writing – review & editing. FF: Data curation, Formal analysis, Methodology, Writing – review & editing. IH: Funding acquisition, Supervision, Writing – review & editing. KA: Funding acquisition, Project administration, Resources, Supervision, Writing – review & editing.

Funding

The author(s) declare that financial support was received for the research, authorship, and/or publication of this article. This study is funded by the Institute of Eminence (IoE), University of Hyderabad for project (UOH/IoE/RC1/20-015) entitled “Sub-seasonal through Interannual Variability of river discharge and its impact on phytoplankton biomass in the Bay of Bengal”.

Acknowledgments

KS acknowledges the director of the National Institute of Oceanography (NIO) in Goa for his immense support. The authors thank the providers of the Godavari River discharge data at Dhavaleswaram, and other data providers for their help in successfully carrying out this study. The authors also thank The International Argo Program and the national initiatives that support it which gathered and made this data publicly available (https://www.ocean-ops.org, https://argo.ucsd.edu). The author thanks Grammarly Free AI tool for Writing Assistance. This is CSIR-NIO contribution number 7313.

Conflict of interest

The authors declare that the research was conducted in the absence of any commercial or financial relationships that could be construed as a potential conflict of interest.

Publisher’s note

Supplementary material

The Supplementary Material for this article can be found online at: https://www.frontiersin.org/articles/10.3389/fmars.2024.1419953/full#supplementary-material

References

Breitburg, D., Levin, L. A., Oschlies, A., Grégoire, M., Chavez, F. P., Conley, D. J., et al. (2018). Declining oxygen in the global ocean and coastal waters. *Science* 359 (6371), p.eaam7240. doi: 10.1126/science.aam7240

Bristow, L. A., Callbeck, C. M., Larsen, M., Altabet, M. A., Dekaezemacker, J., Forth, M., et al. (2017). N2 production rates limited by nitrite availability in the Bay of Bengal oxygen minimum zone. *Nat. Geosci.* 10, 24–29. doi: 10.1038/ngeo2847

Castro-González, M., Molina, V., Rodríguez-Rubio, E., and Ulloa, O. (2014). The first report of a microdiverse anammox bacteria community in waters of Colombian Pacific, a transition area between prominent oxygen minimum zones of the eastern tropical Pacific. *Environ. Microbiol. Rep.* 6, 595–604. doi: 10.1111/1758-2229.12165

Central Water Commission (2019). Status of trace and toxic metals in Indian Rivers. Ministry of Jal Shakti, Department of Water Resources, River Development and Ganga Rejuvenation. 123, 302.

Garcia, H. E., Weathers, K. W., Paver, C. R., Smolyar, I., Boyer, T. P., Locarnini, M. M., et al. (2019). *World Ocean Atlas 2018, Volume 3: Dissolved Oxygen, Apparent Oxygen Utilization, and Dissolved Oxygen Saturation*. A. Mishonov Technical Ed.; NOAA Atlas NESDIS 83, 38.

Gilly, W. F., Beman, J. M., Litvin, S. Y., and Robison, B. H. (2013). Oceanographic and biological effects of shoaling of the oxygen minimum zone. *Annu. Rev. Mar. Sci.* 5, 393–420. doi: 10.1146/annurev-marine-120710-100849

Howden, S. D., and Murtugudde, R. (2001). Effects of river inputs into the Bay of Bengal. *J. Geophysical Research: Oceans* 106, 19825–19843. doi: 10.1029/2000JC000656

Ittekkot, V., Nair, R. R., Honjo, S., Ramaswamy, V., Bartsch, M., Manganini, S., et al. (1991). Enhanced particle fluxes in Bay of Bengal induced by injection of fresh water. *Nature* 351, 385–387. doi: 10.1038/351385a0

Jana, S., Gangopadhyay, A., and Chakraborty, A. (2015). Impact of seasonal river input on the Bay of Bengal simulation. *Continental Shelf Res.* 104, 45–62. doi: 10.1016/j.csr.2015.05.001

Kalvelage, T., Lavik, G., Lam, P., Contreras, S., Arteaga, L., Löscher, C. R., et al. (2013). Nitrogen cycling driven by organic matter export in the South Pacific oxygen minimum zone. *Nat. Geosci.* 6, 228–234. doi: 10.1038/ngeo1739

Marra, J., Ho, C., and Trees, C. (2003). An alternative algorithm for the calculation of primary productivity from remote sensing data. *Deep-Sea Res. I* 54, 155–163.

McCreary, J. P. Jr., Yu, Z., Hood, R. R., Vinaychandran, P. N., Furue, R., Ishida, A., et al. (2013). Dynamics of the Indian-Ocean oxygen minimum zones. *Prog. Oceanography* 112, 15–37. doi: 10.1016/j.pocean.2013.03.002

Naqvi, S. W. A., Shailaja, M. S., Kumar, M. D., and Gupta, R. S. (1996). Respiration rates in subsurface waters of the northern Indian Ocean: Evidence for low decomposition rates of organic matter within the water column in the Bay of Bengal. *Deep Sea Res. Part II: Topical Stud. Oceanography* 43, 73–81. doi: 10.1016/0967-0645(95)00080-1

Notarstefano, G. (2020). *Argo Float Data and Metadata from Global Data Assembly Centre (Argo GDAC)*. doi: 10.17882/42182

O'Reilly, J. E. (2017). *Transboundary Waters Assessment Programme (TWAP), Status and Trends in primary productivity and chlorophyll from 1996 to 2014 in Large Marine Ecosystems and the Western Pacific Warm Pool, based on data from satellite ocean colour sensors* (Paris: IOC-UNESCO).

Paulmier, A., and Ruiz-Pino, D. (2009). Oxygen minimum zones (OMZs) in the modern ocean. *Prog. Oceanography* 80, 113–128. doi: 10.1016/j.pocean.2008.08.001

Pennington, J. T., Mahoney, K. L., Kuwahara, V. S., Kolber, D. D., Calienes, R., and Chavez, F. P. (2006). Primary production in the eastern tropical Pacific: A review. *Prog. oceanography* 69, 285–317. doi: 10.1016/j.pocean.2006.03.012

Ramaiah, N., Fernandes, V., Bhaskar, J., Retnamma, J., Gauns, M., and Jayraj, E. A. (2010). Seasonal variability in biological carbon biomass standing stocks and production. *Indian J. Mar. Sci.* 39 (3), 369–379.

Rao, C. K., Naqvi, S. W. A., Kumar, M. D., Varaprasad, S. J. D., Jayakumar, D. A., George, M. D., et al. (1994). Hydrochemistry of the Bay of Bengal: possible reasons for a different water-column cycling of carbon and nitrogen from the Arabian Sea. *Mar. Chem.* 47, 279–290. doi: 10.1016/0304-4203(94)90026-4

Saha, S., Nadiga, S., Thiaw, C., Wang, J., Wang, W., Zhang, Q., et al. (2006). The NCEP climate forecast system. *J. Climate* 19, 3483–3517. doi: 10.1175/JCLI3812.1

Sarma, V. V. S. S., Jagadeesan, L., Dalabehera, H. B., Rao, D. N., Kumar, G. S., Durgadevi, D. S., et al. (2018). Role of eddies on intensity of oxygen minimum zone in the Bay of Bengal. *Continental Shelf Res.* 168, 48–53. doi: 10.1016/j.csr.2018.09.008

Sarma, V. V. S. S., Prasad, V. R., Kumar, B. S. K., Rajeev, K., Devi, B. M. M., Reddy, N. P. C., et al. (2010). Intra-annual variability in nutrients in the Godavari estuary, India. *Continental Shelf Res.* 30, 2005–2014. doi: 10.1016/j.csr.2010.10.001

Sarma, V. V. S. S., Rao, G. D., Viswanadham, R., Sherin, C. K., Salisbury, J., Omand, M. M., et al. (2016). Effects of freshwater stratification on nutrients, dissolved oxygen, and phytoplankton in the Bay of Bengal. *Oceanography* 29, 222–231. doi: 10.5670/oceanog.2016.54

Sarma, V. V. S. S., and Udaya Bhaskar, T. V. S. (2018). Ventilation of oxygen to oxygen minimum zone due to anticyclonic eddies in the Bay of Bengal. *J. Geophysical Research: Biogeosciences* 123, 2145–2153. doi: 10.1029/2018JG004447

Sathyendranath, S., Brewin, R. J., Brockmann, C., Brotas, V., Calton, B., Chuprin, A., et al. (2019). An ocean-colour time series for use in climate studies: the experience of the ocean-colour climate change initiative (OC-CCI). *Sensors* 19, 4285. doi: 10.3390/s19194285

Sridevi, B., and Sarma, V. V. S. S. (2021). Role of river discharge and warming on ocean acidification and pCO2 levels in the Bay of Bengal. *Tellus B: Chem. Phys. Meteorology* 73, 1–20. doi: 10.1080/16000889.2021.1971924

Udaya Bhaskar, T. V. S., Sarma, V. V. S. S., and Pavan Kumar, J. (2021). Potential mechanisms responsible for spatial variability in intensity and thickness of oxygen minimum zone in the Bay of Bengal. *J. Geophysical Research: Biogeosciences* 126, e2021JG006341. doi: 10.1029/2021JG006341

Zweng, M. M., Reagan, J. R., Seidov, D., Boyer, T. P., Locarnini, R. A., Garcia, H. E., et al. (2018). *World Ocean Atlas 2018, Volume 2: Salinity* Vol. 82. Ed. A. Mishonov (NOAA Atlas NESDIS). 82, 50.